中 国 气 象 局
China Meteorological Administration

国家卫星气象中心
National Satellite Meteorological Centre

FY-3D/MERSI-II and FY-4A/AGRI DCC Calibration Implementation

National Satellite Meteorological Center(NSMC), CMA

Bei Zhang , Xiuqing Hu

September 12 , 2024

中 国 气 象 局
China Meteorological Administration

国家卫星气象中心
National Satellite Meteorological Centre

Content

1、Background

2、Sensors and Data

3、Method

4、Results and Discussion

5、Conclusions and future

1、 Background

- **FY-3D/MERSI-II** and **FY-4A/AGRI** are approaching the end of their designed lifespan, with significant **degradation** of radiometric response in several bands.

- DCC as a invariant Target:

  ✓ Stable Reflectance
  ✓ Easy to Identify
  ✓ Flat Spectrum
  ✓ High Frequency of Occurrence
  ✓ Lambertian
  ✓ Minimal Influence from Water Vapor and Aerosols

- Evaluates the degradation of radiometric response in these two imaging sensors at solar reflective bands(RSB) using DCC target.

FY4B_Cloud_20240903110000 , NSMC

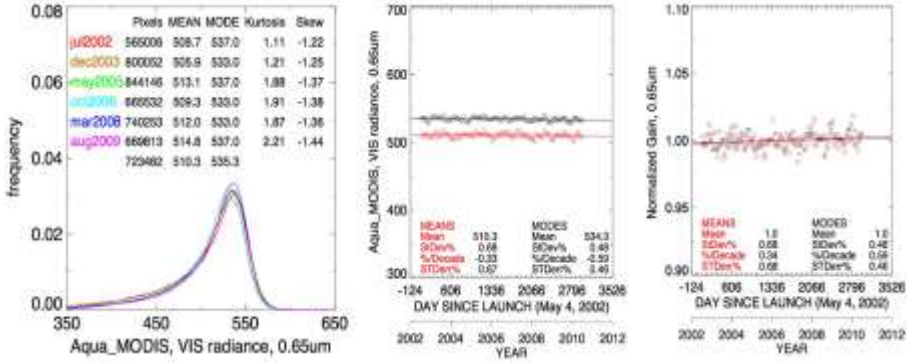

Doelling ,2013

2、Sensors and Data

① FY-3D/MERSI-II

- **Time：20180101~20221231.**
- **Bands：B1-B7、B16-B19.**

3 visible 、5 near-infrared and 3 shortwave infrared bands.

☐ B8 to B15 may **saturate** when observing DCC targets.

Band	Central wavelength (μm)	Spectra bandwidth (μm)	Resolution (m)	Dynamic range
1	**0.470**	50	250	90%
2	**0.550**	50	250	90%
3	**0.650**	50	250	90%
4	**0.865**	50	250	90%
5	**1.38**	20/30	1000	90%
6	**1.64**	50	1000	90%
7	**2.13**	50	1000	90%
8	0.412	20	1000	**30%**
9	0.443	20	1000	**30%**
10	0.490	20	1000	**30%**
11	0.555	20	1000	**30%**
12	0.670	20	1000	**30%**
13	0.709	20	1000	**30%**
14	0.746	20	1000	**30%**
15	0.865	20	1000	**30%**
16	**0.905**	20	1000	100%
17	**0.936**	20	1000	100%
18	**0.940**	50	1000	100%
19	**1.03**	20	1000	100%

solar reflective bands(RSB) of MERSI-II

② FY-4A/AGRI

- **Time：20170301~20230430.**
- **Bands：B1-B6.**

2 visible 、1 near-infrared and 3 shortwave infrared bands.

Band	Central wavelength (μm)	Spectra bandwidth (μm)	Sensitivity
1	**0.470**	0.45~0.49	S/N≥90 @ ρ=100%
2	**0.650**	0.55~0.75	S/N≥200 @ ρ=100%
3	**0.825**	0.75~0.90	S/N≥200 @ ρ=100%
4	**1.375**	1.36~1.39	S/N≥90 @ ρ=100%
5	**1.61**	1.58~1.64	S/N≥200 @ ρ=100%
6	**2.25**	2.1~2.35	S/N≥200 @ ρ=100%
7	3.75	3.5~4(High)	NEΔT≤0.7K @ 300K
8	3.75	3.5~4(Low)	NEΔT≤0.2K @ 300K
9	6.25	5.8~6.7	NEΔT≤0.3K @ 260K
10	7.10	6.9~7.3	NEΔT≤0.3K @ 260K
11	8.50	8.0~9.0	NEΔT≤0.2K @ 300K
12	10.7	10.3~11.3	NEΔT≤0.2K @ 300K
13	12.0	11.5~12.5	NEΔT≤0.2K @ 300K
14	13.5	13.2~13.8	NEΔT≤0.5K @ 300K

3、Method：

➢ **flowchart of the radiometric response assessment method based on DCC ：**

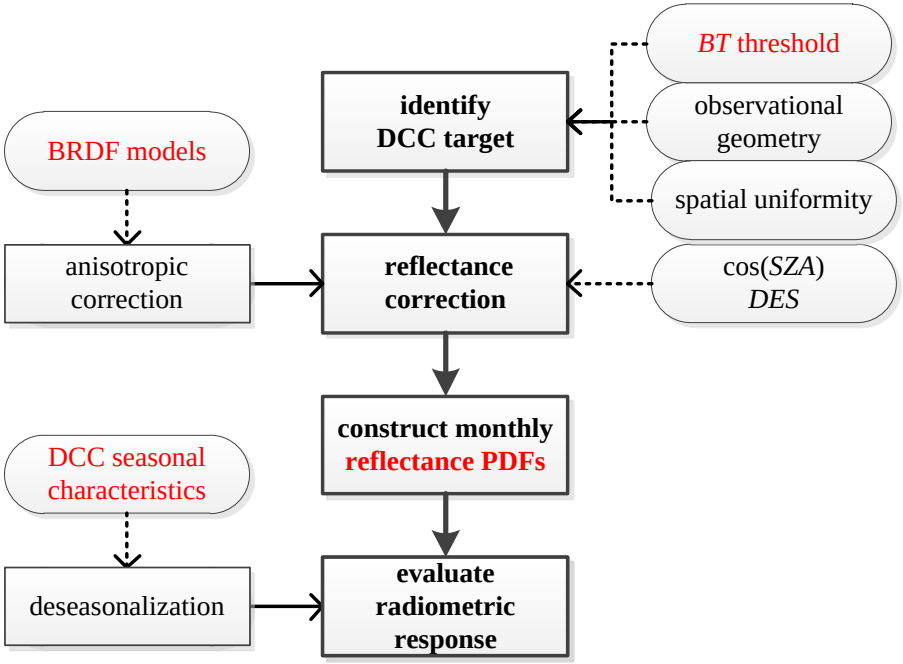

- Factors Affecting the Calibration Accuracy:
  - DCC BRDF characteristic
  - Seasonal Cycles
  - Sensitivity of infrared band threshold and calibration accuracy
  - Mean and mode of DCC reflectance

  .....

D. R. Doelling, D. Morstad, B. R. Scarino, **R. Bhatt,** *et al*. The Characterization of Deep Convective Clouds as an Invariant Calibration Target and as a Visible Calibration Technique. IEEE Transactions on Geoscience and Remote Sensing, vol. 51, no. 3, pp. 1147-1159, March 2013.

Chen L, Hu X, Xu N, *et al*. The Application of Deep Convective Clouds in the Calibration and Response Monitoring of the Reflective Solar Bands of FY-3A/MERSI (Mediμm Resolution Spectral Imager). Remote Sensing. 2013; 5(12):6958-6975.

3、Method：

① Identify DCC target：

Parameter	Threshold
Longitude	-180° ~ +180°
Latitude	-20° ~ +20°
IR BT threshold	**<=205K**
SZA,VZA	<=40°
IR-BT consistency	<=1K
VIS consistency	<=3%

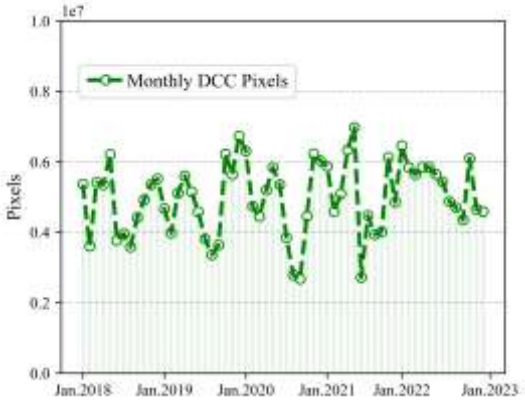

（FY-3D/MERSI-II） Monthly count of DCC pixels

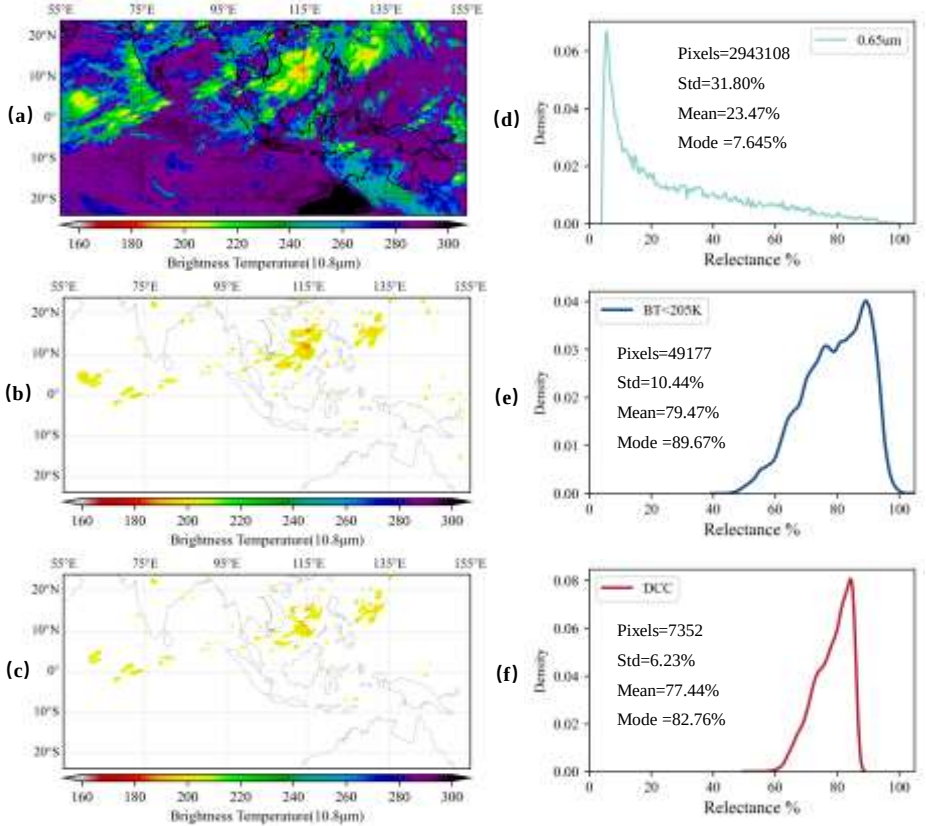

（FY-4A/AGRI）DCC Pixels Identification Process.

(a) All Valid Pixels；(b) Potential DCC Pixels with Infrared Brightness Temperature Less than 205 K；(c) DCC Pixels Filtered by View Angle and Spatial Uniformity Thresholds；(d~f) Corresponding Reflectance PDF for the 0.65 μm band.

3、Method：

② **Reflectance correction**

$$R_i = \frac{D^2 * R^*_i}{\cos(sza) * BRDF(sza, vza, raa)}$$

③ **Construct monthly reflectance PDFs**

④ **Evaluate radiometric response**

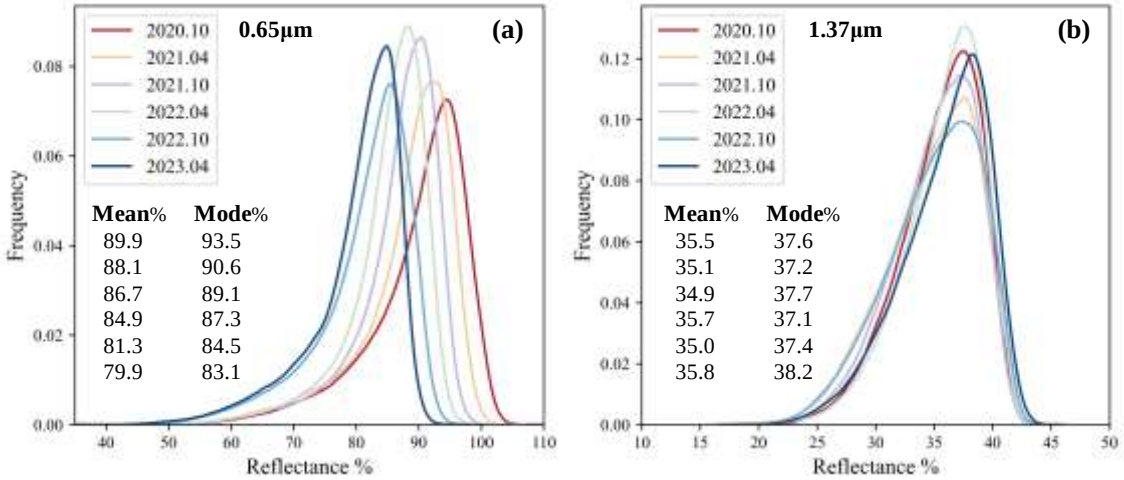

October 2020 to April 2023，(FY-4A/AGRI) DCC Monthly Reflectance PDFs
(a)0.65μm；(b)1.37μm

4、Results and Discussion：

①Sensitivity of Infrared BT Thresholds and Calibration Accuracy

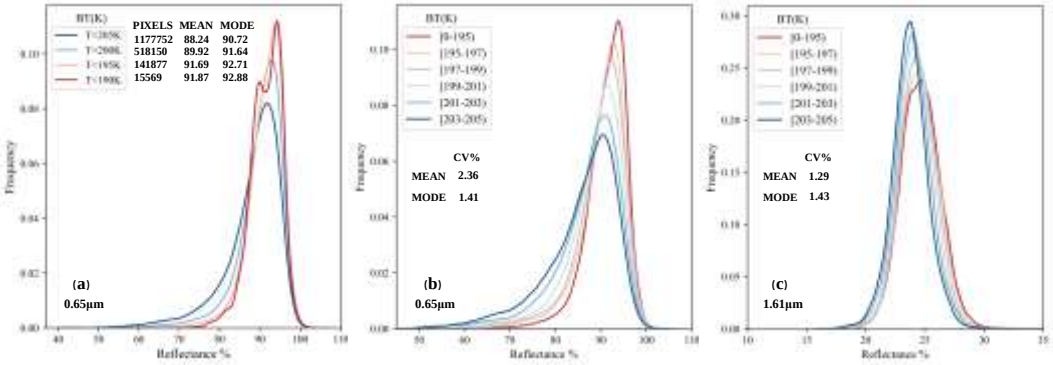

(FY4A/AGRI) DCC Reflectance PDF at Different BT Thresholds.

(a)0.65μm ,190K to 205K；(b) 0.65μm ,195K to 205K；(c)1.61μm, 195K to 205K

a) BT threshold = 190 K, the number of DCC pixels sharply decreases, resulting in an unclear mode of the PDF.

b) The 0.65μm PDF exhibits a left-tailed negatively skewed Gaussian distribution, with the mean being less than the mode.

The coefficient of variation (CV) of the mean is greater than the mode.

c) The 1.61μm exhibits a normal Gaussian distribution, with a mean approximately equal to the mode and **the CV slightly smaller than the mode.**

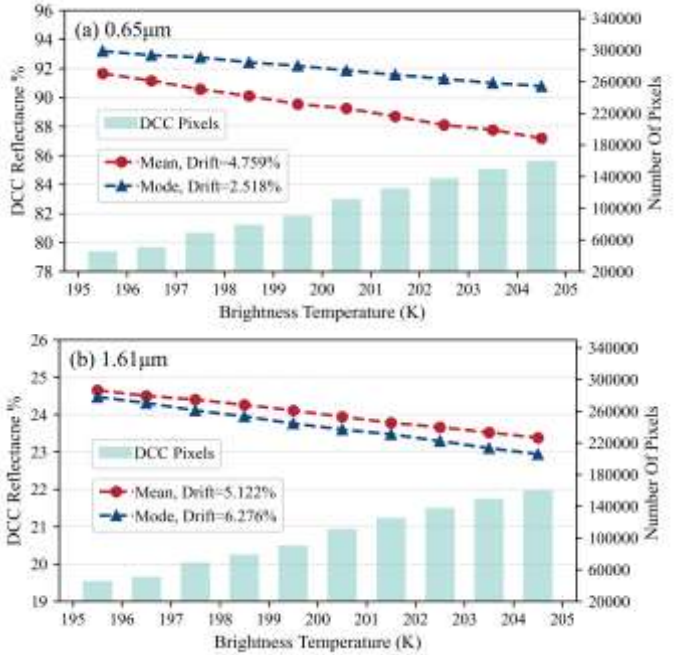

(FY4A/AGRI) Sensitivity of DCC Reflectance Mean and Mode to Infrared band Calibration Accuracy

(a)0. 65μm ; (b)1. 61μm

a) 0.65 μm: The total drift of mean between 195 K and 205 K is 4.76%, while the total drift of the mode is smaller at 2.52%.

The sensitivity of the mode is lower than the mean.

b) 1.61μm: The total drift of mean between 195 K and 205 K is 5.12%, while the total drift of the mode is slightly larger at 6.28%.

The sensitivity of the mean is lower than the mode.

4、Results and Discussion：②Anisotropy Correction: Hu and CERES Thick-Ice-Cloud BRDF Models

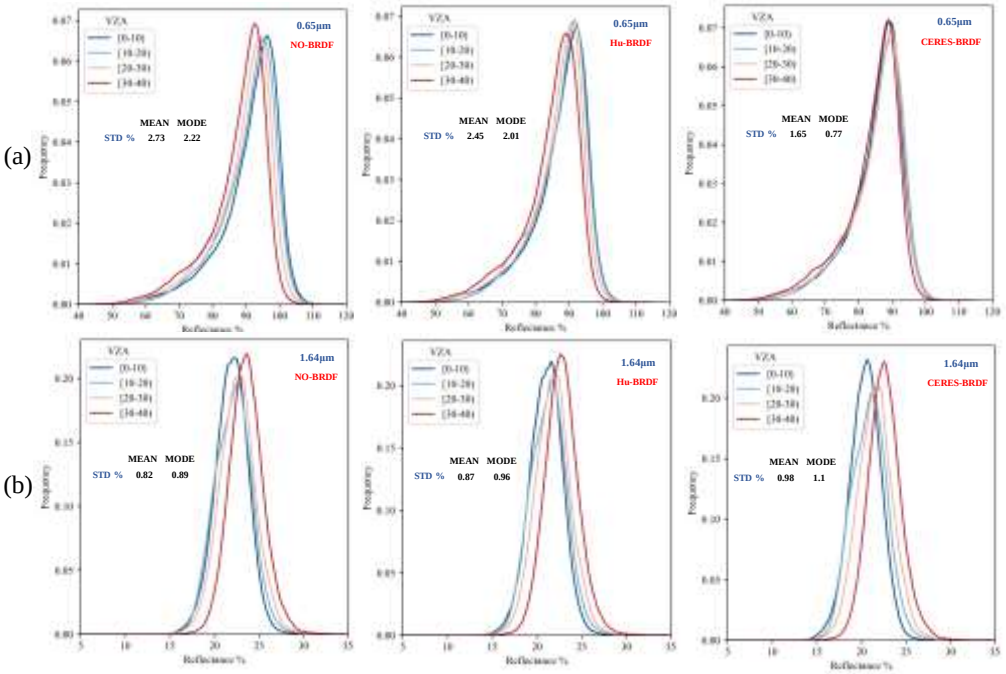

（FY3D/MERSI）DCC Reflectance PDFs for Different VZA Ranges , May 2021

(a)0.65μm (b)1.64μm

➢ **Standard Deviation of the DCC Reflectance Mean (Mode) for Different VZA Ranges**

Band	Central wavelength (μm)	Standard deviation of mean(mode) %		
		No BRDF	Hu BRDF	CERES BRDF
1	0.470	2.32(1.93)	2.22(1.94)	**1.93(0.76)**
2	0.550	2.62(2.13)	2.72(2.11)	**2.33(0.83)**
3	0.650	2.73(2.22)	2.45(2.01)	**1.65(0.77)**
4	0.865	1.63(1.58)	1.53(1.62)	**1.66(0.73)**
5	1.38	0.83(1.08)	1.13(1.28)	**1.16(1.33)**
6	1.64	0.82(0.89)	0.87(0.96)	**0.98(1.1)**
7	2.13	0.76(0.88)	1.26(1.36)	**1.08(1.21)**
16	0.905	1.44(1.28)	1.43(1.12)	**1.41(0.53)**
17	0.936	1.53(1.28)	1.58(1.17)	**1.66(0.73)**
18	0.940	1.22(1.08)	1.37(1.04)	**1.66(0.67)**
19	1.03	1.47(1.13)	1.33(1.02)	**1.67(0.74)**

① **VIS/NIR**: CERES thick-ice-cloud model better than Hu model.

② **SWIR**: Neither model has correction effect.

1、*Hu Y B, Wielicki B A, Yang P, et al. Application of deep convective cloud albedo observation tosatellite-based study of the terrestrial atmosphere: Monitoring the stabilityof spaceborne measurements and assessing absorption anomaly.*

2、*CERES Thick-Ice-Cloud BRDF Models:* ***https://ceres.larc.nasa.gov/data/angular-distribution-models/***

4、Results and Discussion：②Anisotropy Correction: Hu and CERES Thick-Ice-Cloud BRDF Models

➢ **(FY-3D/MERSI) Monthly DCC Reflectance Variation Trends after Correction with Two BRDF Models**

(a) 0.65 μm (b) 1.64 μm

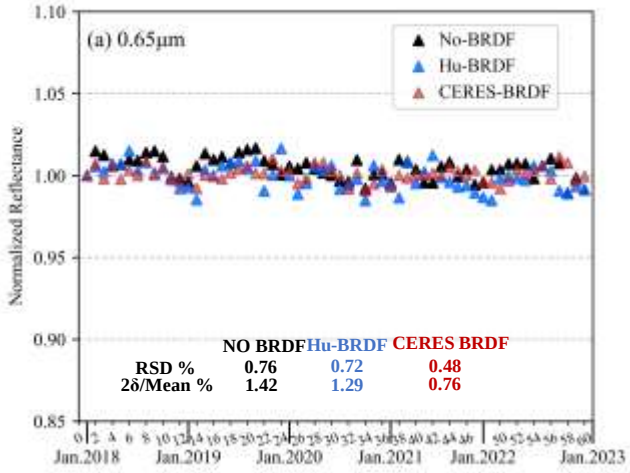

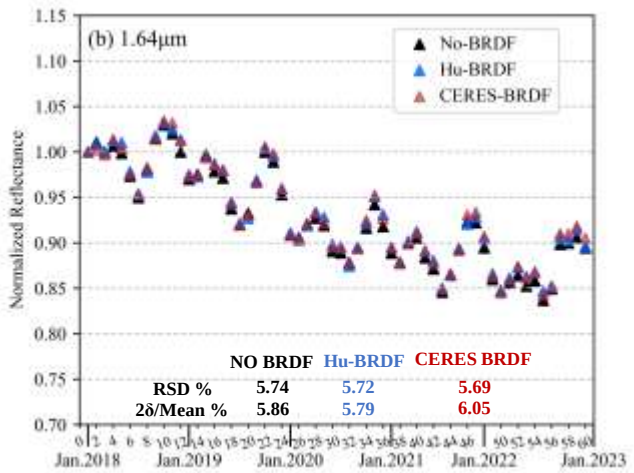

① **VIS/NIR**: After correction with the CERES thick ice cloud model, the reflectance RSD decreased by 15% to 40%, the variability index decreased by 10% to 30%, more effective than Hu model.

② **SWIR:** Neither model has correction effect.

③ 1.64μm exhibits significant periodic variation characteristics, which related to the **seasonal** cycle of DCC.

- **RSD**: Relative Standard Deviation
- **variability index**： 2δ/Mean

  δ=Standard Deviation of Fitting Residuals，

  Mean=mean of Fitted Values.

4、Results and Discussion： ③ DCC Seasonal Characteristics: Global Distribution (FY3D-MERSI)

➢ Distribution of DCC in Tropical Regions for **(a) April** and **(b) July** from 2020 to 2022

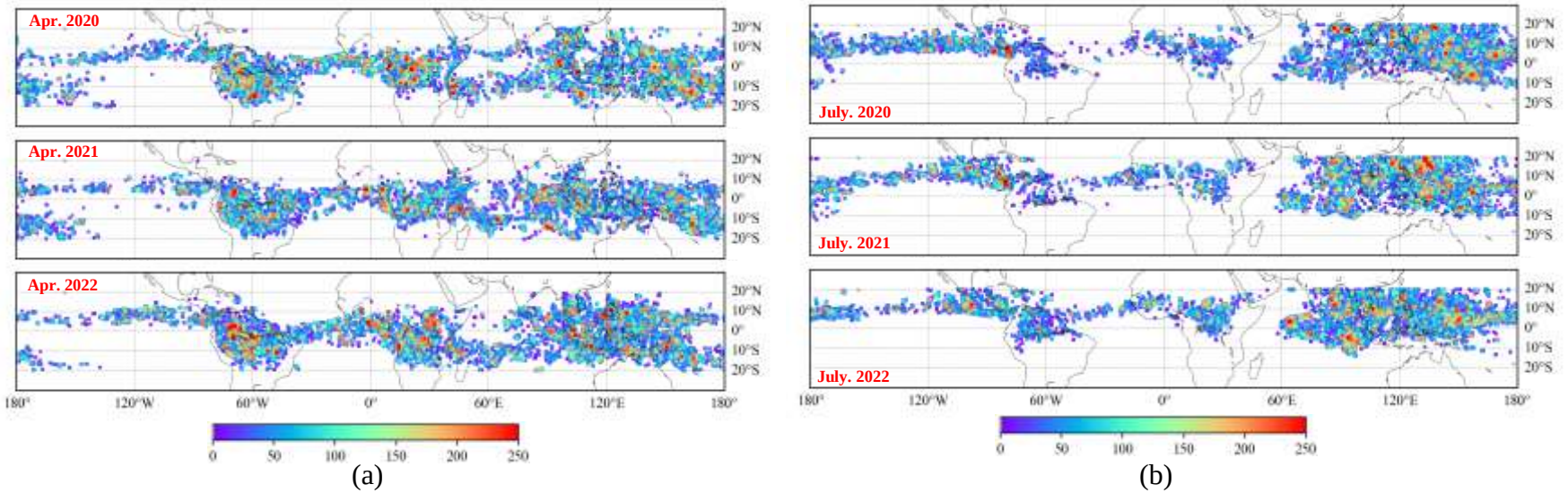

(a) (b)

① The DCC distribution is highly consistent across the same month in different years, while significant differences are observed between different months within the same year.

② Every April, DCC appears more frequently in the Western Pacific, Africa, and South America.

③ Every July, DCC shifts north of the equator, with an average of about 78% of pixels in the northern hemisphere. The frequency of occurrence in Africa and South America has significantly decreased, with about 70% of pixels appearing in the western Pacific and Indian Ocean regions.

④ **DCC reflectance is different over ocean and land**. (Rajendra B, 2017.)

4、Results and Discussion：③ DCC Seasonal Characteristics: Annual cycle of DCC Reflectance

➢ Annual Variation of Monthly DCC Reflectance for **(a) 1.64 μm** and **(b) 2.13 μm** from 2018 to 2022 (FY-3D/MERSI)

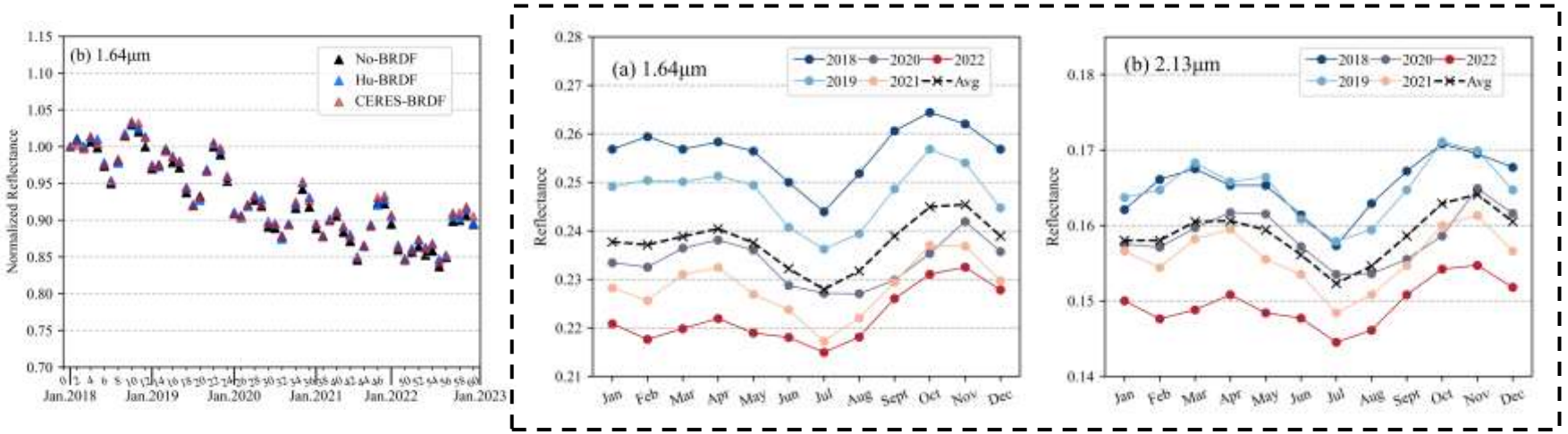

① **SWIR** : The DCC reflectance decreases annually.

② Monthly trend of DCC reflectance is similar each year, minimum values in February and July, maximum values in April and October.

③ The annual average variation range of monthly reflectance in VIS/NIR bands is 1.5%, **while the reflectance in the SWIR bands shows higher sensitivity to seasonal variation**, with an average variation range of about 6.4%.

4、Results and Discussion：

③ DCC Seasonal Characteristics: Seasonal index(SI)

Uses a simple ratio-to-moving-average method that is performed in four steps:

① A 12-month centered running mean is computed.

② Then, a relative ratio between the actual month value and the running mean is determined.

③ Next, an average relative ratio for each month is computed, which is known as seasonal index (SI).

④ Finally, the DCC modes are divided by month-specific SIs to yield seasonally adjusted time series.

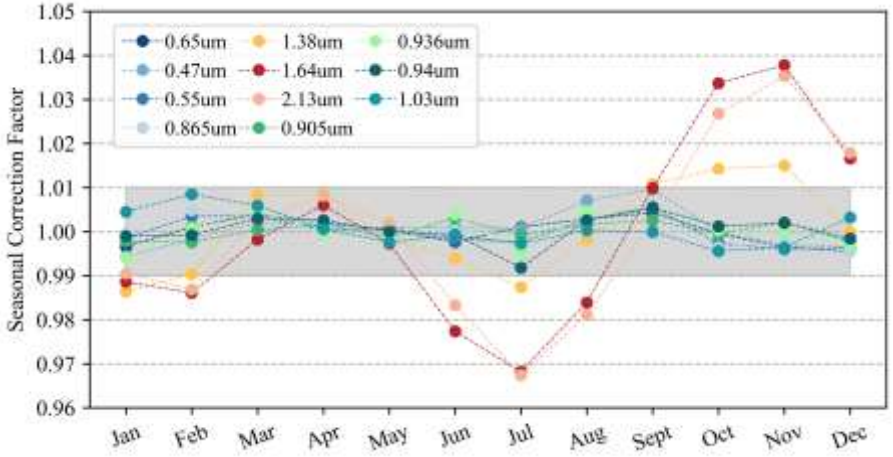

Seasonal Index (SI) of DCC

① The seasonal index(SI) is positively correlated with the magnitude of seasonal fluctuations in DCC reflectance.

② VIS/NIR bands, the variation range of SI within 2%, while in the SWIR bands, the variation range increases to 7%, indicating greater seasonal sensitivity.

Rajendra B , David D , Benjamin S , *et al*. Development of Seasonal BRDF Models to Extend the Use of Deep Convective Clouds as Invariant Targets for Satellite SWIR-Band Calibration[J]. Remote Sensing, 2017, 9(10):1061.

4、Results and Discussion：③ DCC Seasonal Characteristics： Deseasonalization Effect

➢ Comparison of Deseasonalization Methods and BRDF Model Correction Results (FY-3D/MERSI)

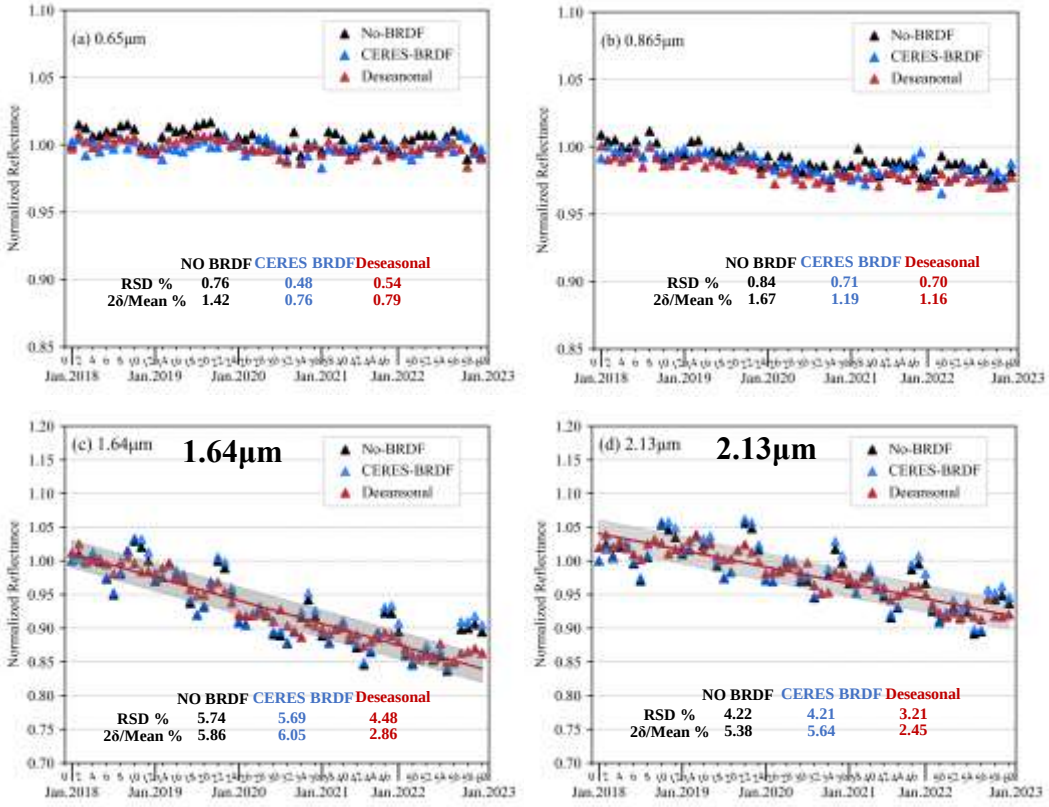

➢ Decline Rates of RSD and Variability Indicators of Reflectance in Each band After deseasonalization (FY-3D/MERSI)

Spectral bands(μm)	Decline Rate of RSD %	Decline Rate of 2δ/Mean %
0.470	10.3	29.9
0.550	9.6	27.3
0.650	28.9	44.3
0.865	16.7	30.5
1.38	22.4	52.7
1.64	22.0	51.2
2.13	23.9	54.5
0.905	17.6	33.5
0.936	18.3	35.6
0.940	18.1	32.4
1.03	20.4	42.8

After deseasonalization , The reflectance RSD of **SWIR** bands decreased by 22.4%, 22.0%, and 23.9%, while the variability index decreased by 52.7%, 51.2%, and 54.5%, respectively.

4、Results and Discussion：④ FY-3D/MERSI-II Degradation Assessment Results

➢ **Normalized Monthly Reflectance of DCC (FY-3D/MERSI-II from 2018 to 2022)**

(a)VIS；(b)NIR；(c)SWIR

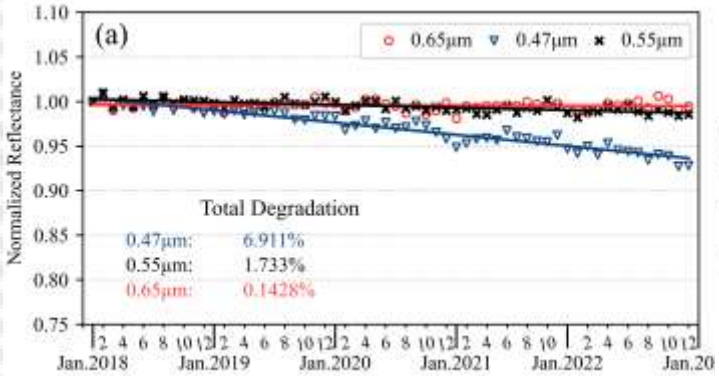

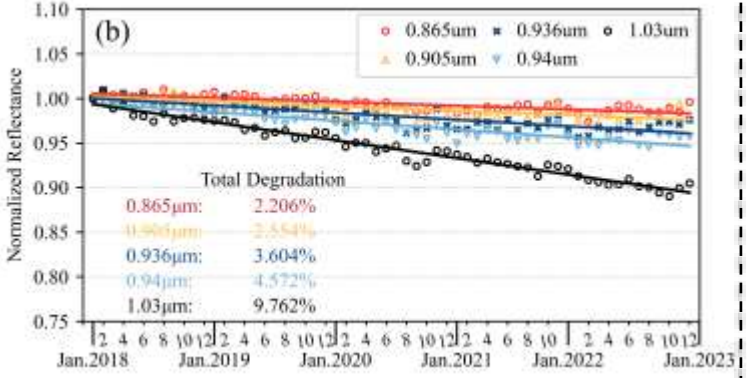

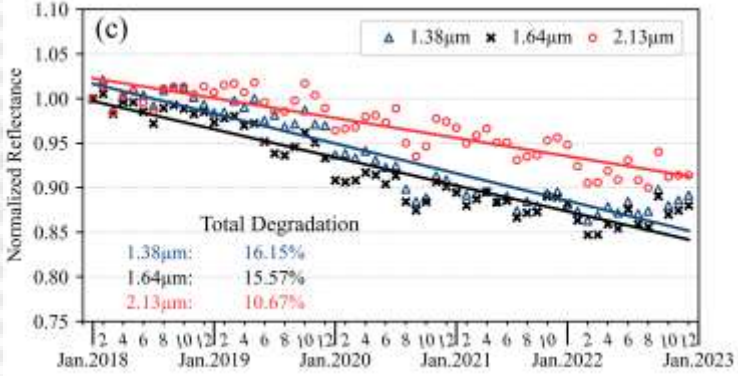

Band	Central wavelength μm	Reflectance mean	Total degradation rate(%)	Annual degradation rate(%)	σ (%)
1	0.470	0.8999	6.911	1.382	1.174
2	0.550	0.8853	1.733	0.3466	0.9643
3	0.650	0.8957	0.1428	0.02856	0.9640
4	0.865	0.9178	2.206	0.4412	1.064
5	1.38	0.5023	16.15	3.231	4.012
6	1.64	0.2248	15.57	3.114	3.565
7	2.13	0.1501	10.67	2.134	3.167
16	0.905	0.8617	2.554	0.5108	1.727
17	0.936	0.7571	3.604	0.7208	2.531
18	0.940	0.8424	4.572	0.9144	2.985
19	1.03	0.8223	9.762	1.952	1.191

➢ **Validation of Multi-site calibration method**

Band	CW μm	Drift(%/yr) DCC	Drift(%/yr) Muti-site
1	0.47	1.38	1.67
2	0.55	0.35	0.47
3	0.65	0.03	0.04
4	0.865	0.44	0.47
5	1.38	3.32	3.08
6	1.64	3.11	2.81
7	2.13	2.13	1.82
16	0.905	0.51	0.81
17	0.936	0.72	0.95
18	0.94	0.91	1.26
19	1.03	1.95	1.82

4、Results and Discussion：④ FY-4A/AGRI Degradation Assessment Results

➢ **Normalized Monthly Reflectance of DCC (FY-4A/AGRI from Apr. 2017 to May 2023)**

(a) VIS / NIR；(b) SWIR

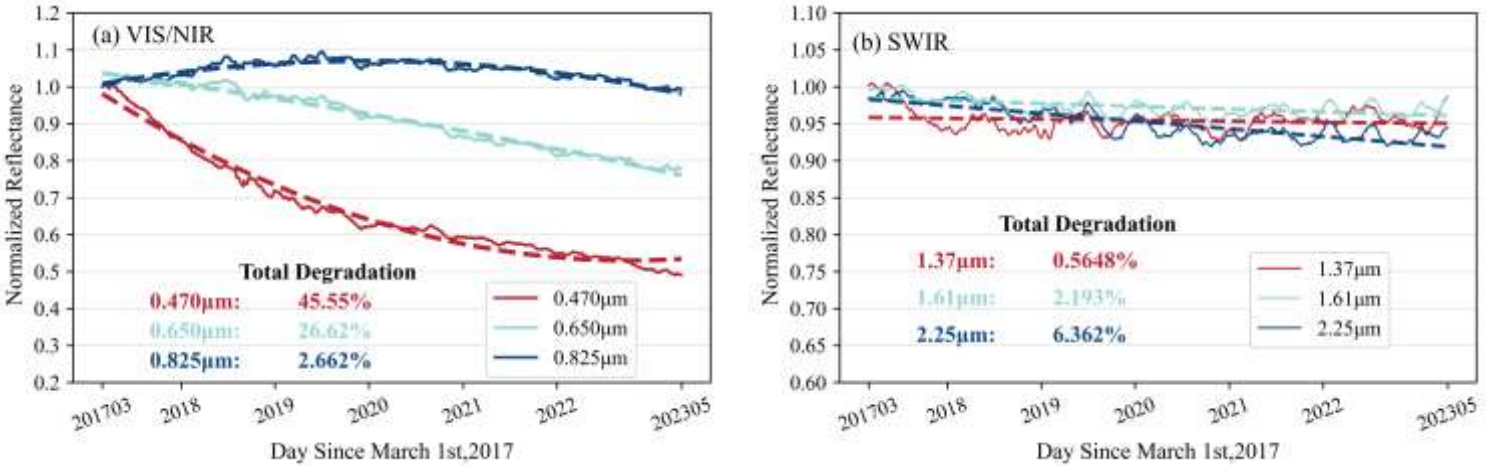

Band (μm)	Total Degradation (%)	Annual Degradation (%)	δ (%)
0.470	45.55	7.383	2.149
0.650	26.62	4.315	1.141
0.865	2.662	0.4314	0.9366
1.375	0.5648	0.0915	1.673
1.61	2.193	0.3556	1.127
2.25	6.362	1.031	1.289

a) **VIS**: Significant degradation with a total rate of 45.55% in 0.47μm. The 0.65μm exhibits a linear trend of degradation, with a total rate of 26.62%.

b) **SWIR**: 1.37μm band degrade by 5% during the first year of launch. 1.61μm and 2.25μm exhibit a linear trend. These three bands has similar periodic fluctuation characteristics, which may be related to the **temperature change** of the sensor.

5、Summary

- DCC is an excellent invariant target for post-launch radiometric calibration of satellite sensors.
- DCC exhibits obvious seasonal characteristics, and the deseasonalization method can reduce the reflectance fluctuations in the SWIR bands.

➢ Future：

- Cross-calibration between polar-orbiting (FY-3) and geostationary(FY-4) satellites.
- Characteristics of DCC reflectance over land and ocean.

➢ Issue：

- DCC seasonal and wavelength dependent BRDF models.
- Separate seasonal cycles and sensor temperature dependence.

Reference

[1] **Rajendra B** , **David D** , Benjamin S , *et al*. Development of Seasonal BRDF Models to Extend the Use of Deep Convective Clouds as Invariant Targets for Satellite SWIR-Band Calibration[J]. Remote Sensing, 2017, 9(10):1061.

[2] **Bhatt** R, **Doelling D**, Wu, A. Initial Stability Assessment of S-NPP VIIRS Reflective Solar Band Calibration Using Invariant Desert and Deep Convective Cloud Targets. Remote Sens. 2014

[3] **Bhatt R , Doelling D R** , Scarino B R , *et al*. Advances in utilizing tropical deep convective clouds as a stable target for on-orbit calibration of satellite imager reflective solar bands[C]// Earth Observing Systems XXIV. 2019.

[4] Fougnie B **, D Doelling**, Crespin A , *et al*. Bidirectional Reflectance Distribution Function (BRDF) of Deep Convective Clouds (DCC) Derived from PARASOL Measurements and Compared to Radiative Transfer Computation and Model[J].2014.

[5] **D. R. Doelling**, D. Morstad, B. R. Scarino, **R. Bhatt,** *et al*. The Characterization of Deep Convective Clouds as an Invariant Calibration Target and as a Visible Calibration Technique. IEEE Transactions on Geoscience and Remote Sensing, vol. 51, no. 3, pp. 1147-1159, March 2013.

[6] Hu Y B, Wielicki B A, Yang P, *et al*. Application of deep convective cloud albedo observation tosatellite-based study of the terrestrial atmosphere: Monitoring the stabilityof spaceborne measurements and assessing absorption anomaly. IEEE Trans. Geosci. Remote Sens., vol. 42, no. 11, pp. 2594–2599, Nov. 2004.

[7] Wang W H, Cao C, Shao X, *et al*. Evaluation of 10-Year NOAA/NASA Suomi NPP and NOAA-20 VIIRS Reflective Solar Band (RSB) Sensor Data Records (SDR) over Deep Convective Clouds. Remote. Sens. 14 (2022): 3566.

[9] Chen L, Hu X, Xu N, *et al*. The Application of Deep Convective Clouds in the Calibration and Response Monitoring of the Reflective Solar Bands of FY-3A/MERSI (Mediμm Resolution Spectral Imager). Remote Sensing. 2013; 5(12):6958-6975.

[10] Wang W, Cao C. Monitoring the NOAA Operational VIIRS RSB and DNB Calibration Stability Using Monthly and Semi-Monthly Deep Convective Clouds Time Series. Remote Sens. 2016, 8, 32.

[11] Wang W and Cao C. Evaluation of NOAA-20 VIIRS Reflective Solar Bands Early On-Orbit Performance Using Daily Deep Convective Clouds Recent Improvements. IEEE Journal of Selected Topics in Applied Earth Observations and Remote Sensing, vol. 13, pp. 3975-3985, 2020.

中 国 气 象 局
China Meteorological Administration

国家卫星气象中心
National Satellite Meteorological Centre

Thanks

for your attention!